

Three-Dimensional Analysis of Nonhuman Primate Trabecular Architecture Using Micro-Computed Tomography

R.J. Fajardo^{1*} and R. Müller²

¹*Interdepartmental Doctoral Program in Anthropological Sciences, State University of New York at Stony Brook, Stony Brook, New York 11794-4364*

²*Orthopedic Biomechanics Laboratory, Beth Israel Deaconess Medical Center and Harvard Medical School, Boston, Massachusetts 02215*

KEY WORDS μ CT methodology; cancellous bone; degree of anisotropy; proximal humerus; proximal femur

ABSTRACT Until recently, detailed analyses of the architecture of nonhuman primate cancellous bone have not been possible due to a combination of methodological constraints, including poor resolution imaging or destructive protocols. The development of micro-computed tomography (μ CT) and morphometric methods associated with this imaging modality offers anthropologists a new means to study the comparative architecture of cancellous bone. Specifically, μ CT will allow anthropologists to investigate the relationship between locomotor behavior and trabecular structure. We conducted a preliminary study on the trabecular patterns in the proximal humerus and femur of *Hylobates lar*, *Ateles paniscus*, *Macaca mulatta*, and *Papio anubis* to investigate the quantitative differences in their trabecular architecture and evaluate the potential of μ CT in anthropological inquiry. μ CT allows the researcher to evaluate variables beyond simple two-dimensional orientations and radio-

graphic densities. For example, this methodology facilitates the study of trabecular thickness and bone volume fraction using three-dimensional data. Results suggest that density-related parameters do not reliably differentiate suspensory-climbing species from quadrupedal species. However, preliminary results indicate that measurements of the degree of anisotropy, a measure of trabecular orientation uniformity, do distinguish suspensory-climbing taxa from more quadrupedal species. The μ CT method is an advance over conventional radiography and medical CT because it can accurately resolve micron-sized struts that make up cancellous bone, and from these images a wide array of parameters that have been demonstrated to be related to cancellous bone mechanical properties can be measured. Methodological problems pertinent to any comparative μ CT study of primate trabecular architecture are discussed. *Am J Phys Anthropol* 115: 327–336, 2001. © 2001 Wiley-Liss, Inc.

Primate trabecular bone architecture continues to be a topic of interest to functional morphologists (Oxnard and Yang, 1981; Heller, 1989; Rafferty and Ruff, 1994; Rafferty, 1996, 1998; Galichon and Thackeray, 1997; Macchiarelli et al., 1999; Rook et al., 1999). Micro-computed tomography (μ CT) is a new imaging tool to visualize trabecular architecture that is superior to the previously used methods of histological sectioning, planar radiography, and medical computed tomography (CT). μ CT generally does not require destructive specimen preparation (but this depends on the bone specimen to gantry size) and can produce images with resolution in the tens of microns. The high-resolution imaging is a critical advance of μ CT over previously used methods, as studies have demonstrated that accurate assessments of trabecular architecture are dependent on image resolution (Engelke et al., 1996; Müller et al., 1996; Kothari et al., 1998). For example, it has been shown that medical CT cannot reliably reproduce trabecular architecture because its resolution limits are commonly equal to or greater than the thickness of an individual trabecula (Engelke et

al., 1996; Müller et al., 1996). In addition, quantitative methods now exist that permit researchers to measure a primate's bony lattice in three dimensions (Odgaard et al., 1990; Odgaard, 1997; Hildebrand and Rüeggsegger, 1997a,b; Smit et al., 1998; Ding et al., 1999), acquiring data on parameters such as bone volume fraction, structural anisotropy (a measure of the extent to which trabeculae are similarly aligned), trabecular thickness, and trabecular separation, to name a few. The bone volume fraction and structural anisotropy are particularly important variables because they are known to impact the mechanical properties of cancellous bone

Grant sponsor: L.S.B. Leakey Foundation; Grant sponsor: National Science Foundation; Grant number: BCS-9904925.

*Correspondence to: Roberto José Fajardo, Department of Anatomical Sciences, State University of New York at Stony Brook, Stony Brook, NY 11794-8081. E-mail: rfajardo@ic.sunysb.edu

Received 23 May 2000; accepted 3 May 2001.

(e.g., Rice et al., 1988; Turner et al., 1990; Ulrich et al., 1999).

Layton et al. (1988) and Feldkamp et al. (1989) first introduced μ CT to the field of bone biology in the late 1980s. Since then, μ CT has primarily been applied to the study of human bone diseases such as osteoporosis. The use of μ CT in the study of comparative primate morphology and functional skeletal analyses has been very limited. Spoor et al. (1994) and Spoor and Zonneveld (1995) first used μ CT imaging in anthropology to study the primate inner ear. Thompson and Illerhaus (1998) recently published another study of the inner ear that focused on hominid samples. To date, there have not been any published comparative μ CT studies of nonhuman primate cancellous bone. The potential of this untapped resource for revealing new information about the relationship between locomotor patterns and trabecular architecture is great, given the established accuracy of μ CT imaging (Müller et al., 1998; Ding et al., 1999) and the recent developments of three-dimensional quantitative methods (Odgaard et al., 1990; Odgaard, 1997; Hildebrand and Rüeggsegger, 1997a,b; Smit et al., 1998; Ding et al., 1999).

We conducted a preliminary analysis on a limited anthropoid sample to examine the potential of μ CT in functional studies of primate trabecular architecture and to explore the methodological issues pertinent to such a study. μ CT and μ CT-based morphometric methods were used to compare the architectural features of trabecular bone among four anthropoid species that vary in locomotor behavior. This analysis focused on two skeletal sites (proximal humerus and proximal femur) in two suspensory-climbing primate species and two quadrupedal species. We chose these locomotor modes to determine whether a variable and nonrepetitive locomotor style like climbing (Fleagle, 1976) produces an architecture different from that of a repetitive, stereotypical gait like quadrupedalism (Jenkins and Camazine, 1977). Differences in the trabecular architecture of suspensory-climbing taxa and quadrupedal taxa are to be expected, because trabecular trajectories and the degree of trabecular bone anisotropy are correlated with orientation and degree of anisotropy of a bone's loading regime (Lanyon, 1974; Goldstein et al., 1991; Biewener et al., 1996). For example, anisotropic trabeculae (structures in which the majority of trabeculae are similarly oriented) appear to result from loads being applied in one to a few orientations, while isotropic trabeculae (structures in which trabeculae are not uniformly oriented) result from loads being applied in many different directions. We therefore expected the trabecular architecture of the proximal humerus and femur to exhibit less structural anisotropy in suspensory taxa, since these elements are believed to be exposed to variable, nonrepetitive loading environments. The same bony regions in the quadrupedal species should exhibit greater structural anisotropy, since this locomotor mode involves repetitive, stereotypical limb excursions

and presumably higher compressive loads on the limbs.

MATERIALS AND METHODS

One humerus and one femur of the species *Hyllobates lar*, *Ateles paniscus*, *Macaca mulatta*, and *Papio anubis* were extracted from wet (preserved in formalin), wild-collected specimens kept at the State University of New York at Stony Brook. All specimens were male and adult, as judged by epiphyseal fusion of the humeral and femoral proximal ends. None of the specimens showed external signs of fracture or markers indicating a bone disorder (e.g., osteophytes).

These four species exemplify a grade in locomotor styles. The gibbon is a below-branch arm-swinger and vertical climber (Fleagle, 1976). The spider monkey engages in suspensory and climbing behaviors similar to the gibbon, but uses quadrupedal postures and locomotion equally as much (Mittermeier, 1978; Cant, 1986). The macaque and baboon are two closely related quadrupedal cercopithecoid monkeys (Rawlins, 1976; Rose, 1977). These two species differ, however, in their substrate use. *M. mulatta* is known to be active in the trees and on the ground, with preference for a terrestrial setting later in life (Rawlins, 1976). According to Rose (1977), *P. anubis* is primarily terrestrial. These species broadly represent the midsize range of primate body sizes (Smith and Jungers, 1997).

During this exploratory study, we used a micro-computed tomography system specifically designed for the analysis of small human bone biopsy samples.¹ Small cores of bone had to be extracted from the proximal humeri and femora of our anthropoid sample, because these specimens were much larger than the gantry of the imaging system. We extracted column-shaped bone cores not exceeding 16 mm in diameter (the size limit of scanner's gantry). They were taken from the humeral and femoral heads, starting at the center of the head inferiorly and proceeding distally, parallel to the long axis of each bone's neck. The inferior and proximal surfaces of the humeral and femoral cores corresponded to the inferior and proximal periosteal surfaces of the bones (external surface). The anatomical planes were marked on each specimen and then matched to the scanner's imaging planes.

μ CT imaging

A desktop μ CT20 imaging system (Scanco Medical, Bassersdorf, Switzerland; Rüeggsegger et al., 1996) was used to image the primate samples. This machine's accuracy was recently tested against histological samples of human trabecular bone, and results indicate that it produces highly accurate im-

¹A few scanners with larger gantries, which can accommodate the skeletal elements of medium and large-bodied primates without sectioning, are currently available for academic research. See Discussion.

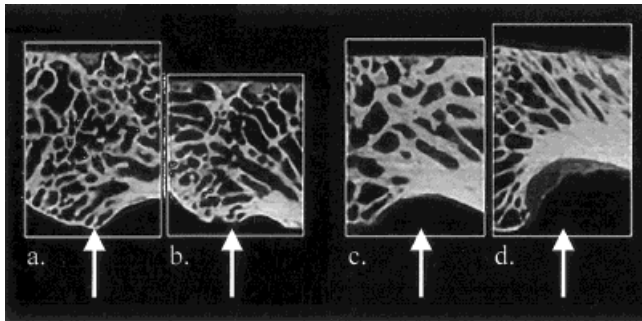


Fig. 1. Two-dimensional μ CT images of nonhuman primate cancellous bone. Proximal humeri of (a) *Hylobates lar* and (b) *Macaca mulatta* are shown in the sagittal plane. Proximal femora of (c) *Hylobates lar* and (d) *Papio anubis* are viewed in the coronal plane. Arrows indicate anatomical landmarks used to center our scans and determine volumes of interest: inferior boundary of the humeral articular surface (a, b) and the most superior point on the curvature of the inferior femoral neck (c, d).

ages (Müller et al., 1998). Samples were scanned at a nominal resolution of $34\ \mu\text{m}$ in all planes (x , y , z). This resolution is adequate to accurately reconstruct trabecular microstructure in μ CT images (Kuhn et al., 1990; Engelke et al., 1996; Müller et al., 1998; Kothari et al., 1998).

We used digital x-ray scout views to locate the regions to be scanned (sagittal view for humerus, frontal view for femur). Anatomical landmarks aided us in identifying these scanning regions. In the proximal humerus, the anatomical landmark consisted of the inferior edge of the proximal humeral articular surface, while in the proximal femur we used the most superior point along the inferior femoral neck's curvature as a landmark. Eight millimeters were scanned in both the humeral and femoral samples, centering all scans on the landmarks (Fig. 1a,b). Prior to morphometric analysis, volumes of interest (VOI) needed to be defined. In the software Structure Analysis Program, spherical volumes of interest are defined using views from the three perpendicular planes. We sampled spherical VOIs in the proximal humerus between the inferior articular boundary on one side and the image's edge anteriorly. Cortical bone was excluded from VOIs by placing the inferior aspect of the sphere superior to the inferior cortex, where trabecular bone was clearly present (Fig. 1a). In the proximal femur, the spherical VOIs were positioned in the head-neck transition region, using the most superior point in the neck curvature as a distal boundary and the image's edge proximally. These VOIs were placed approximately 25 slices inferior to the bone's cut plane superiorly (Fig. 1b). These volumes of interest were not scaled according to body size, even though our sample does show at least a twofold increase in body size (*Papio* compared to the other three taxa). Location and scaling of VOIs are complex issues in comparative studies of trabecular bone; these issues are treated in the Discussion.

Images were thresholded prior to morphometric analysis. Thresholding is the process of binarizing

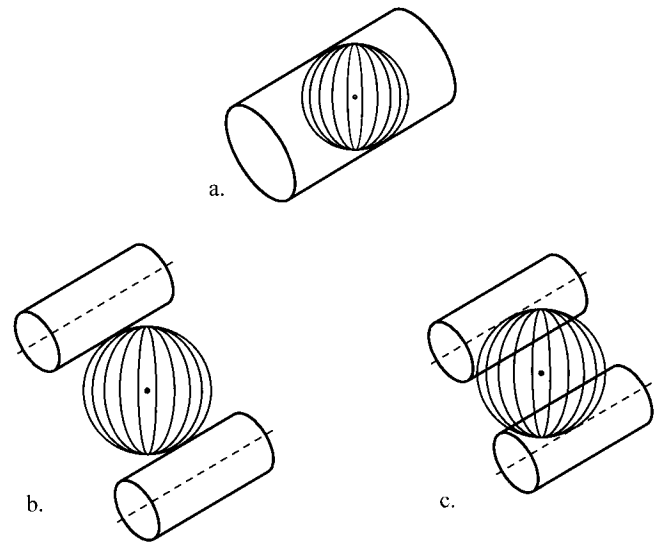


Fig. 2. Measurements of (a) average trabecular thickness (Tb.Th), (b) trabecular separation (Tb.Sp), and (c) trabecular number (Tb.N). Spheres are used in the three-dimensional image to calculate Tb.Th, Tb.Sp, and Tb.N.

an image (black and white) to distinguish bone from the surrounding marrow cavity. We applied a threshold protocol established by Müller et al. (1998) in which each individual image's threshold is set to 10.2% of its maximal gray value.

Quantitative bone morphometry

Measurements of bone volume fraction, trabecular number, trabecular thickness, trabecular separation, and degree of anisotropy were made on all specimens. These measurements were automated, using software developed for the desktop μ CT20 system (for a comprehensive description, see Hildebrand and Rüegsegger, 1997b; Müller et al., 1998; Hildebrand et al., 1999). We will only briefly describe these methods here. The bone volume fraction (BV/TV) is a ratio of the volume of bone present (BV) to the total volume of interest (TV). Trabecular thickness (Tb.Th) is measured by placing non-overlapping spheres within the trabeculae that are centered on the midaxis of each strut (Fig. 2a). The average diameter of all spheres placed within the trabeculae is the average trabecular thickness of the volume (Hildebrand and Rüegsegger, 1997b). Trabecular separation (Tb.Sp) is measured by fitting non-overlapping spheres of maximal diameter to the marrow spaces (Fig. 2b). A slight variation of this method is used to calculate trabecular number (Tb.N). Non-overlapping spheres are placed in the VOI, using the midaxes of the struts as the boundaries. The mean trabecular number is defined as the inverse of the average diameter of all spheres placed between the midaxes of the trabeculae (Fig. 2c; and see Hildebrand et al., 1999).

We used the mean intercept length (MIL) to measure the anisotropy of the trabeculae in the VOI (Whitehouse, 1974; Harrigan and Mann, 1984). To

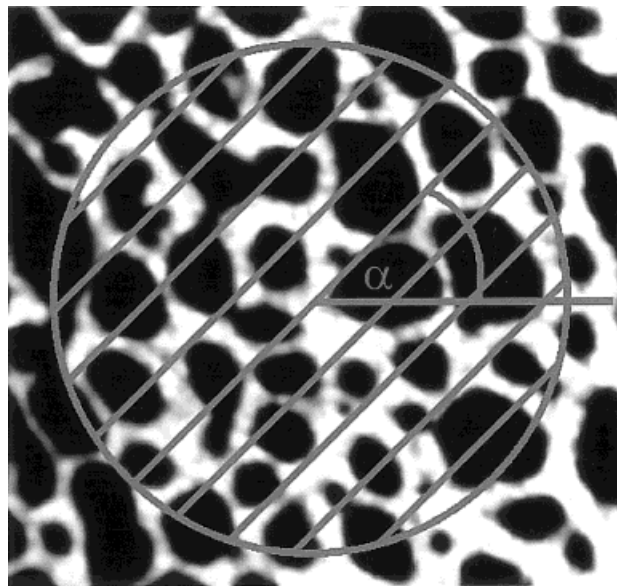


Fig. 3. Example of a test grid used to calculate the mean intercept length (MIL). To determine MIL for any image plane, the average distance between two bone-marrow interfaces is counted. The MIL is determined for several rotations of the grid through 180° on randomly selected images.

calculate the MIL, a circular grid of parallel test lines is superimposed on images of trabecular bone in each of the three image axes, x, y, and z (Fig. 3). The average distance between bone-marrow cavity interfaces is calculated by counting the number of interfaces along the test lines and dividing that sum by the length of all lines in the test grid. This yields the mean intercept length. Subsequently, the grid is rotated 5° with respect to an arbitrary axis on the image, and the counts are repeated in angular increments of 5° through 180° for all three scan axes. These counts create a series of values in the form MIL (α_i), where α is the angle at which the count was taken (0°–180°) with respect to a reference axis, and i is the scan plane of the image (= x, y, or z scan planes which are orthogonal to each other). In this implementation, 49 randomly distributed images from the x, y, and z scan planes were analyzed. These MIL (α_i) data are fit to the function of an ellipsoid (Harrigan and Mann, 1984). The degree of anisotropy of the trabecular architecture (MIL-DA) is defined as the ratio of the primary axis to the tertiary axis of the MIL ellipsoid (Goulet et al., 1994). At ratios close to 1, the axes are of similar value and the bone structure is isotropic. As the ratio increases above 1, the degree of anisotropy of the bone increases.

RESULTS

Table 1 lists the results of density-related measurements for both the proximal humerus and proximal femur, along with data collected by Beddoe (1978) on *Macaca*, which will be discussed later. Proximal humerus BV/TV was very similar among the four species of primates, with the values ranging

between 29–35%. Measurements of the Tb.Th, Tb.Sp, and Tb.N overlapped between the four taxa in our sample. In the proximal femur, the BV/TV values were more spread out, with values ranging between 46–77%. The quadrupedal taxa occupied the high end of the range and the suspensory taxa the low end, but the difference between lowest value for the quadrupeds and the highest value for the two suspensory species was only 5%. All four primates had trabeculae in the proximal femur that ranged in thickness between 0.170–0.200 mm, with values overlapping between the two locomotor groups. Tb.N also overlapped between the two locomotor groups in our sample, with values ranging between 0.93/mm–1.59/mm. The average distance between trabeculae was smaller in *Macaca* and *Papio* by at least 0.120 mm.

MIL-DA results indicated that *Hylobates* and *Ateles* have less anisotropic trabeculae in the proximal humerus than do *Macaca* and *Papio*. The 1.12 and 1.18 values for *Hylobates* and *Ateles*, respectively, are very near the 1.00 minimum value possible in MIL-DA analyses, which characterizes a completely isotropic structure (Table 2). Two- and three-dimensional images of the *Hylobates* and *Macaca* proximal humerus visually reinforce the structural differences indicated by the MIL-DA (Figs. 1a,b, 4). In the proximal femur, the values are absolutely higher for all taxa, but again the MIL-DA values are lower in the two suspensory-climber species than in the quadrupedal taxa. However, even though the suspensory species are three-dimensionally less anisotropic, both groups exhibited a pattern of superomedially radiating trabeculae in the coronal plane. This point is demonstrated by *Hylobates* and *Papio* in Figures 1c,d and 5.

DISCUSSION

In this study, our goal was to investigate the trabecular architecture of two anthropoid locomotor groups and, through this study, examine the μ CT method. In the following discussion, we will briefly discuss our preliminary results and some methodological issues that we faced during this research and that others will face during similar comparative studies.

Our results suggest that degree of anisotropy of anthropoid trabecular architecture correlates with locomotor behavior in a predictable way. *Hylobates* and *Ateles*, which presumably place more variable loads on their joints due to their locomotor habits, have less anisotropic trabeculae than *Macaca* and *Papio*, in both the proximal humerus and proximal femur. It appears that the repetitive nature of the quadrupedal gait and the stereotypical loads this locomotor mode engenders are associated with a greater structural anisotropy in both proximal limb bone regions. This relationship between loading regimes and trabecular orientation has some support from biomechanical theory and experimental MIL-DA data (e.g., Goldstein et al., 1991).

TABLE 1. Results of analyses of four trabecular bone-density related parameters¹

Species	Site	BV/TV (%)	Tb.Th (mm)	Tb.Sp (mm)	Tb.N (1/mm)
<i>Hylobates lar</i>	Humerus	34.0	0.190	0.366	1.80
	Femur	58.0	0.472	0.336	1.24
<i>Ateles paniscus</i>	Humerus	29.0	0.182	0.449	1.58
	Femur	46.0	0.339	0.391	1.37
<i>Macaca mulatta</i>	Humerus	35.0	0.196	0.367	1.78
	Femur	77.0	0.824	0.247	0.93
<i>Papio anubis</i>	Humerus	35.0	0.167	0.301	2.10
	Femur	64.0	0.400	0.229	1.59
<i>Macaca</i> sp. (from Beddoe, 1978)	Humerus	30.6	0.201	0.401	
	Femur	40.1	0.284	0.424	

¹ BV/TV, bone volume fraction; Tb.Th, average trabecular thickness; Tb.Sp, average trabecular spacing; Tb.N, average trabecular number.

TABLE 2. Results of the MIL-DA analysis for the proximal humerus and proximal femur

Species	Humerus	Femur
<i>Hylobates lar</i>	1.12	1.35
<i>Ateles paniscus</i>	1.18	1.47
<i>Macaca mulatta</i>	1.44	1.78
<i>Papio anubis</i>	1.28	1.62

Alternatively, our results imply that measurements of density-related variables in the proximal humerus and proximal femur do not reliably discriminate between primate locomotor groups. *Macaca* and *Papio* did have higher BV/TV values in the proximal femur than their suspensory counterparts, but we feel that the 5% difference between the baboon and the gibbon is not solid enough evidence to jump to this conclusion. However, it is interesting to note that bone density is the most important determinant of cancellous bone strength (Turner et al., 1990; Martin, 1991; Turner 1992; Ulrich et al., 1999), and BV/TV, which is a surrogate measure of bone density (Rice et al., 1988), was higher in the quadrupedal anthropoids.

Comparison of the two trabecular bone data sets revealed an interesting interlimb structural pattern. The proximal humerus, in general, had a lower BV/TV. In concert with this lower BV/TV, the struts of the proximal humerus were thinner, more distantly spaced, and found in greater number, regardless of the locomotor behavior. This pattern holds true for the humerus of a forelimb-dominated animal, like *Hylobates*, and the quadrupedal *Papio*. This result gains support from two other studies that made interlimb structural comparisons (Beddoe, 1978; Rafferty, 1996). Beddoe (1978) showed in a two-dimensional histological study that the humerus has lower BV/TV and thinner trabeculae than the femur (see Table 1). However, unlike our own results, Beddoe (1978) found the intertrabecular spacing was higher in the femur. In a much broader sampling of primates, Rafferty (1996) also reported that trabecular bone density, as measured from two-dimensional radiographs, was higher in the femoral head than in the humeral head, regardless of locomotor mode.

Due to our small sample size, we were not able to quantitatively analyze the allometry of trabecular architectural parameters. However, no size-trend is apparent. The overlapping thicknesses between species in our sample that differ in body size corroborate the results of prior studies of trabecular architecture, which indicate that parameters of trabecular architecture are independent of body size (Mullender et al., 1996; Swartz et al., 1998).

In discussing the μ CT methodology presented here, the first question that must be asked is whether the method provides any more information than current x-ray imaging methods. Indeed, more can be learned about the three-dimensional structure of trabecular bone with μ CT than with planar radiography or medical CT. Neither of these two conventional alternatives can accurately measure the variables reported in this study, due to either their poor imaging resolution or restriction to two-dimensional imaging. For example, some medical CT scanners can reach a maximum resolution of 0.250 mm, but the resolution more commonly ranges between 0.500–1 mm. Our nonhuman primate Tb.Th data indicate that a single voxel error in a medical CT scan will, at best (i.e., at 0.250 mm), result in the complete loss of a trabecula in humeral images and between 30–74% error in Tb.Th measurements of the proximal femur. Planar radiography also is not a viable option, since it produces two-dimensional, low-resolution summation images (objects superimposed on each other in the image) that may visually misrepresent the variability in trabecular orientation and anisotropy (Whitehouse and Dyson, 1974).

Accurate two- and three-dimensional trabecular morphometry is possible with histological techniques (e.g., Swartz et al., 1998; Kothari et al., 1998). However, this method is, by its nature, destructive at all times. In large-scale studies, histological techniques or any imaging methodology that requires destructive specimen preparation is not an option for anthropologists, since extinct and extant primate skeletal materials are scarce. While the combination of our interest in medium-sized anthropoid trabecular architecture and the use of the Scanco20 μ CT scanner required us to section our

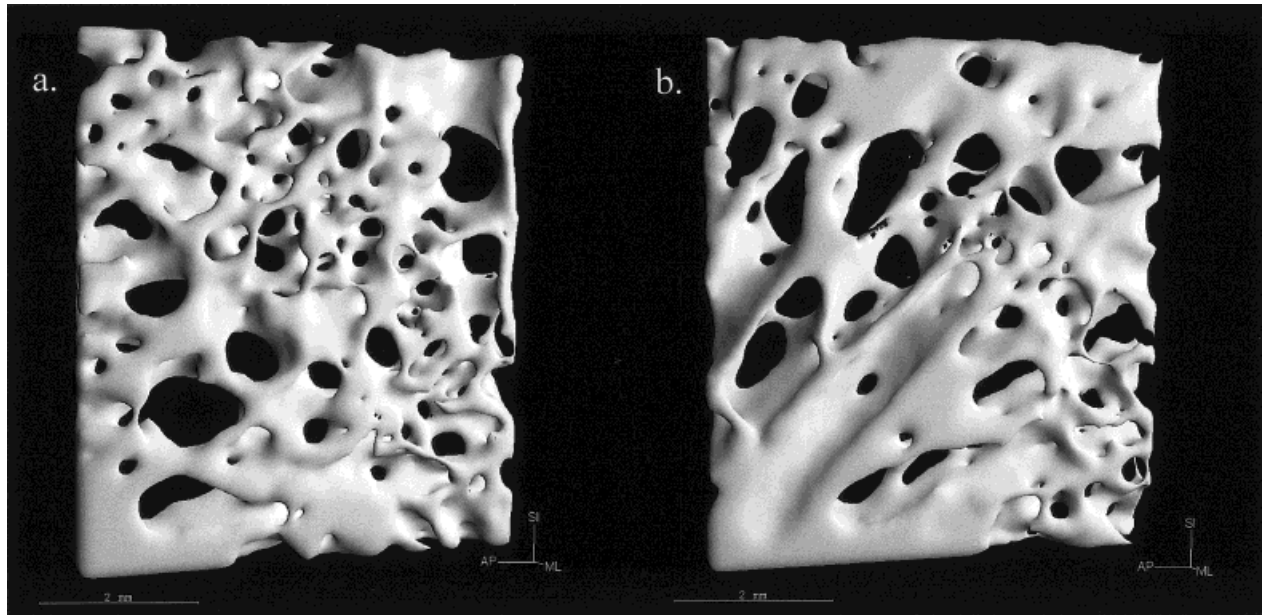


Fig. 4. Three-dimensional reconstructions of nonhuman primate humeral cancellous bone. **a:** *Hylobates lar* (10 sagittal slices in image). Note near-isotropic structure of trabeculae. **b:** *Macaca mulatta* (8 sagittal slices in image). Trabeculae of *Macaca* show a higher degree of anisotropy, with preferential orientation in the superoposterior direction. In both images, posterior is towards the right of the image.

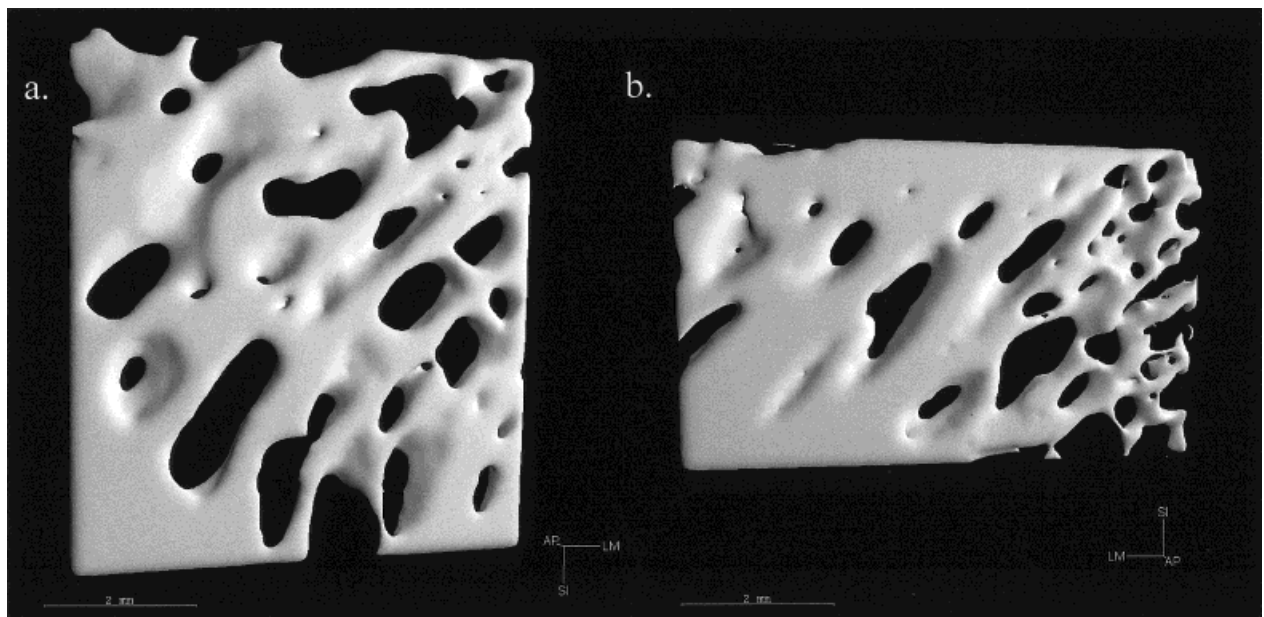


Fig. 5. Three-dimensional reconstructions of nonhuman primate femoral cancellous bone. Medial is to the right of the image. **a:** *Hylobates lar* (5 coronal slices in image). **b:** *Papio anubis* (5 coronal slices in image). Suspensory primates have less structural anisotropy in the proximal femur, but all four individuals exhibit a pattern of superomedially radiating trabeculae.

specimens, as we stated earlier, the μ CT method can be nondestructive so long as the size of the bones in the sample are smaller than the gantry's size dimensions. The Scanco20 scanner's gantry size limits objects to a maximum diameter of 16 mm. This gantry size makes it perfect for nondestructive analyses of small-bodied strepsirhines, such as *Galago* and *Perodicticus* (Fajardo et al., 2000), or callitrichids. Nondestructive studies of medium to large-bodied

primates will require high-resolution scanners with larger gantry sizes, such as the one currently in use at the University of Texas at Austin (Fajardo et al., 1999; Ryan, 2000), which accepts specimens of up to 500 mm in diameter by 750 mm in length. The Ford Motor Company has another large gantry system (Brochu, 1999), but the University of Texas system appears to be the only one used primarily for academic research in the United States.

In future comparative studies of trabecular architecture, researchers should carefully consider the numerous factors known to influence trabecular architecture when planning their study samples. Ample human data exist which suggest that trabecular bone density is influenced by age, gender, reproductive status, hormone levels, and state of health (e.g., nutrition, disease; Aaron et al., 1985; Mellish et al., 1989; Crane et al., 1990; Kneissel et al., 1994; Kalkwarf and Specker, 1995; Majumdar et al., 1997; Parsons et al., 1997). These same variables do not appear to affect the structural geometry as much (Geraets et al., 1997; Mosekilde, 1989). The data on how these factors influence nonhuman primate bone quality are slowly growing, especially on macaques, but remain limited (DeRousseau, 1985; Pope et al., 1989; Grynopas et al., 1993; Kammerer et al., 1995; Cahoon et al., 1996; Champ et al., 1996; Lees and Jerome, 1998; Ott et al., 1999; Cerroni et al., 2000). It appears that age adversely affects nonhuman primate bone density, particularly in females (the effect on males, if any, is still unclear; DeRousseau, 1985; Pope et al., 1989; Cahoon et al., 1996; Champ et al., 1996; Cerroni et al., 2000), but there appears to be some debate about the effect of the reproductive cycle on female nonhuman primate bone (Lees and Jerome, 1998; Ott et al., 1999). More data need to be collected, especially across a greater diversity of primate taxa, but until then, comparative study samples should be designed taking into consideration factors such as age, gender, and disease.

Two factors that must be considered very carefully prior to any analysis of trabecular architecture are the location of the VOIs and their size. It has already been demonstrated that trabecular architecture variables can vary over short distances in humans (Whitehouse and Dyson 1974; Whitehouse, 1975). For example, in the human femoral head, stereological measurements of BV/TV can vary between 12–37% depending on the location of the VOI (Whitehouse and Dyson, 1974). In fact, they show that repositioning the VOI in the same individual only a few millimeters in another direction can result in a BV/TV change between 1–13%. In the human femoral head, MIL-DA and Tb.Th measurements can also fluctuate greatly, depending on the location of the VOI (Whitehouse and Dyson, 1974). However, this trabecular architectural variation does appear to correspond with theoretical stress models of the human proximal femur (e.g., Pauwels, 1960). BV/TV, Tb.Th, and MIL-DA values tend to be elevated in the medial compressive band of trabeculae. If we assume a similar amount of variation in nonhuman primates, then it is imperative that researchers make every effort to identify anatomically as well as biomechanically homologous VOIs.

The results of this analysis must be considered preliminary not only due to the small sample size but also because the VOIs were not scaled according to body size. The gantry's size limits, in combination with the shape of the individual bones, prohibited us

from scaling the VOIs according to body size. However, it is interesting to note that although VOIs were not scaled and there is at least a twofold difference in body size between *Papio* and *Macaca*, these two taxa exhibit similar trabecular architectures.

It is important to point out that choosing to scale or not scale VOIs has consequences that merit consideration. First, if VOIs are uniform across a sample with a large range in body size, you might expect to be “oversampling” the smaller species and thereby not necessarily comparing biomechanically similar regions. However, growing evidence indicates that average trabecular thicknesses do not vary greatly across mammals (Mullender et al., 1996; Swartz et al., 1998). If this is the case, then scaling VOIs across taxa in a study group may lead to a sampling bias. More trabeculae will be sampled and measured in larger taxa than in smaller taxa. In a sample including *Microcebus*, *Gorilla*, and species in between these two body sizes, for example, it would not be an exaggeration to state that only 10–15 trabeculae might be sampled in the *Microcebus* femur, while hundreds of trabeculae would be sampled in the *Gorilla* femur. Assuming that the intraindividual architectural variability across small regions is also great in nonhuman primates, then we can expect the results to have much larger standard deviations in the small species. Nevertheless, the goal of comparative trabecular architectural studies is to analyze biomechanically homologous regions, and it is only through the scaling of VOIs that this can be achieved. We strongly recommend that VOIs be scaled according to body size or some local, biomechanically relevant dimension. For instance, we scale the VOIs according to femoral neck lengths in a current study, using a larger sampling of anthropoids.

Another issue to consider is the method of quantifying the degree of anisotropy. The MIL method is the most commonly used technique (e.g., Teng and Herring, 1995; Martin et al., 1998), but it has been criticized by some authors because it is unable to correctly characterize two-dimensional structural test patterns in all cases (Odgaard et al., 1990; Kuo and Carter, 1991; Geraets, 1998; Smit et al., 1998). Furthermore, some researchers question the process of fitting the MIL (α) data to the function for an ellipsoid (or an ellipse in two-dimensional analyses) because it limits the characterization of orientation to only perpendicular axes (Kuo and Carter, 1991), when it is clear that trabeculae do not always intersect at right angles (the major axis identifying the primary orientation of the trabeculae, and the minor axis identifying secondary orientations in the structure; Pauwels, 1960; Lanyon, 1974; Oxnard and Yang, 1981).

A couple of alternatives to the MIL-DA exist. These alternative methods are the volume orientation (VO) and the star volume distribution (SVD) method (Odgaard et al., 1990, 1997; Smit et al.,

1998). In brief, these three-dimensional methods work by determining the directions in which more bone tissue exists. A recent test comparing the MIL-DA, VO, and SVD methods showed that the VO and SVD are slightly better measures of the degree of anisotropy, since they correlate more highly with the mechanical properties of trabecular bone (Odgaard et al., 1997). However, the researchers concluded that all three anisotropy methods reliably predicted the mechanical main directions of the testing samples and produced similar results.

We chose to use the MIL method, which is the first step in calculating the degree of anisotropy (see Materials and Methods), because there is a demonstrated relationship between MIL-DA values and the mechanical properties of bone. First, the MIL-DA and the anisotropy of Young's modulus are correlated, with the planes of greater structural organization coinciding with those of greater stiffness (Turner et al., 1990). Although the relationship between the orientation as determined with MIL-DA values and ultimate strength has not yet been studied, early work by Galante et al. (1970) showed that the qualitatively determined main orientation of cancellous bone corresponded to the plane of greatest ultimate strength in mechanical tests. Second, after bone density or some surrogate measurement of it (e.g., BV/TV), anisotropy, as determined by MIL-DA, is the second most important variable for explaining the mechanical behavior of cancellous bone. In fact, when these two variables are combined, over 92% of the variance in yield strength and 70–82% of the variance in Young's modulus can be explained (Turner, 1992; Ulrich et al., 1999). In our opinion, the demonstrated relationship between MIL-DA and the mechanical behavior of cancellous bone justifies its use in comparative studies of cancellous bone. MIL-DA is able to capture the functional signal of trabecular architecture, which, in the end, is our goal.

In summary, this preliminary μ CT analysis of primate trabecular architecture demonstrates that this technique has the potential to reveal greater detail about the functional structure of nonhuman primate cancellous bone than previously known. The approach presented here offers several benefits for physical anthropologists. First, it permits a rigorous quantitative treatment of interspecific differences in nonhuman primate trabecular architecture. Second, it allows the analysis of local volumes within a bone which, when sampled across many sites within a bone, can be related to models of bone loading. Third, although we extracted cores of bone from whole samples in this study, such a protocol is not necessary and is primarily determined by the dimensions of each scanner's gantry. Finally, previous successes in visualizing the internal structure of primate fossils using medical CT and μ CT allude to the possibility of using μ CT to study the trabecular architecture of extinct primates (Tate and Cann, 1982; Conroy and Vannier, 1984; Spoor et al., 1994;

Galichon and Thackeray, 1997; Joeckel, 1998; Thompson and Illerhaus, 1998).

ACKNOWLEDGMENTS

The authors thank Brigitte Demes for her insightful comments and help in improving this manuscript. R.J.F. also thanks G. Hébert for her editorial comments and support, and C. Heesy and P. O'Connor for enlightening discussions and technical support. This work and future research on cancellous bone by R.J.F. are supported by grants from the L.S.B. Leakey Foundation and the National Science Foundation (BCS-9904925).

LITERATURE CITED

- Aaron JE, Makins NB, Sagreya K. 1987. The microanatomy of trabecular bone loss in normal aging men and women. *Clin Orthop* 215:260–271.
- Beddoe AH. 1978. A quantitative study of the structure of trabecular bone in man, rhesus monkey, beagle, and miniature pig. *Calcif Tissue Res* 25:273–281.
- Biewener AA, Fazzalari NL, Konieczynski DD, Baudinette RV. 1996. Adaptive changes in trabecular architecture in relation to functional strain patterns and disuse. *Bone* 19:1–8.
- Brochu CA. 1999. High-resolution CT analysis of a *Tyrannosaurus rex* skull. *J Vert Paleont [Suppl]* 19:34.
- Cahoon S, Boden SD, Gould KG, Vailas AC. 1996. Noninvasive markers of bone metabolism in the rhesus monkey: normal effects of age and gender. *J Med Primatol* 25:333–338.
- Cant JGH. 1986. Locomotion and feeding postures of spider and howling monkeys: field study and evolutionary interpretation. *Folia Primatol (Basel)* 46:1–14.
- Cerroni AM, Tomlinson GA, Turnquist JE, Grynpsas MD. 2000. Bone mineral density, osteopenia, and osteoporosis in the rhesus macaques of Cayo Santiago. *Am J Phys Anthropol* 113:389–410.
- Champ JE, Binkley N, Havighurst T, Colman RJ, Kemnitz JW, Roecker EB. 1996. The effects of advancing age on bone mineral content of female rhesus monkeys. *Bone* 5:485–492.
- Conroy GC, Vannier MW. 1984. Noninvasive three-dimensional computer imaging of matrix-filled fossil skulls by high-resolution computed tomography. *Science* 226:456–458.
- Crane GJ, Fazzalari NL, Parkinson IH, Vernon-Roberts B. 1990. Age-related changes in femoral trabecular bone arthropathy. *Acta Orthop Scand* 61:421–426.
- DeRousseau CJ. 1985. Aging in the musculoskeletal system of rhesus monkeys: III. Bone loss. *Am J Phys Anthropol* 68:157–167.
- Ding M, Odgaard A, Hvid I. 1999. Accuracy of cancellous bone volume fraction measured by micro-CT scanning. *J Biomech* 32:323–326.
- Engelke K, Song SM, Gluer CC, Genant HK. 1996. A digital model of trabecular bone. *J Bone Miner Res* 11:480–489.
- Fajardo RJ, Ryan TM, Kappelman J. 1999. Quantitative analysis of primate trabecular bone architecture: comparison of high-resolution x-ray computed tomography and histologic sections. *Am J Phys Anthropol [Suppl]* 28:125.
- Fajardo RJ, MacLatchy LM, Müller R. 2000. Analysis of femoral head trabecular architecture using μ CT: evidence from some anthropoids and lorisooids. *Am J Phys Anthropol [Suppl]* 30:147.
- Feldkamp LA, Goldstein SA, Parfitt AM, Jesion G, Kleerekoper M. 1989. The direct examination of three-dimensional bone architecture *in vitro* by computed tomography. *J Bone Miner Res* 4:3–11.
- Fleagle JG. 1976. Locomotion and posture of the Malayan siamang and implications for hominoid evolution. *Folia Primatol (Basel)* 26:245–269.
- Galante J, Rostoker W, Ray RD. 1970. Physical properties of trabecular bone. *Calcif Tissue Res* 5:236–246.

- Galichon V, Thackeray JF. 1997. CT scans of trabecular bone structure in the ilia of Sts 14 (*Australopithecus africanus*), *Homo sapiens* and *Pan paniscus*. *S Afr J Sci* 93:179–180.
- Geraets WGM. 1998. Comparison of two methods for measuring orientation. *Bone* 23:383–388.
- Geraets WGM, Van der Stelt PF, Lips P, Elders PJM, Van Ginkel FC, Burger EH. 1997. Orientation of the trabecular pattern of the distal radius around the menopause. *J Biomech* 4:363–370.
- Goldstein SA, Matthews LS, Kuhn JL, Hollister SJ. 1991. Trabecular bone remodeling: an experimental model. *J Biomech* 24:135–150.
- Goulet RW, Goldstein SA, Ciarelli MJ, Kuhn JL, Brown MB, Feldkamp LA. 1994. The relationship between the structural and orthogonal compressive properties of trabecular bone. *J Biomech* 27:375–389.
- Grynopas MD, Hancock RGV, Greenwood C, Turnquist JE, Kessler MJ. 1993. The effects of diet, age, and sex on the mineral content of primate bones. *Calcif Tissue Int* 52:399–405.
- Harrigan TP, Mann RW. 1984. Characterization of microstructural anisotropy in orthotropic materials using a second rank tensor. *J Materials Sci* 19:761–767.
- Heller JA. 1989. Stress trajectories in the proximal femur of archaic *Homo sapiens* and modern humans. *Am J Phys Anthropol [Suppl]* 78:239.
- Hildebrand T, Rügsegger P. 1997a. Quantification of bone microarchitecture with the structure model index. *Comput Methods Biomech Biomed Eng* 1:15–23.
- Hildebrand T, Rügsegger P. 1997b. A new method for the model-independent assessment of thickness in three-dimensional images. *J Microsc* 185:67–75.
- Hildebrand T, Müller R, Laib A, Dequeker J, Rügsegger P. 1999. Direct three-dimensional morphometric analysis of human cancellous bone: microstructural data from spine, femur, iliac crest, and calcaneus. *J Bone Miner Res* 14:1167–1174.
- Jenkins FA, Camazine SM. 1977. Hip structure and locomotion in ambulatory and cursorial carnivores. *J Zool Lond* 181:351–370.
- Joeckel RM. 1998. Unique frontal sinuses in fossil and living Hyaenidae (Mammalia, Carnivora): description and interpretation. *J Vert Paleont* 18:627–639.
- Kalkwarf HJ, Specker BL. 1995. Bone mineral loss during lactation and recovery after weaning. *Obstet Gynecol* 86:26–32.
- Kammerer CM, Sparks ML, Rogers J. 1995. Effects of age, sex and heredity on measures of bone mass in baboons (*Papio hamadryas*). *J Med Primatol* 24:236–242.
- Kneissel M, Boyde A, Hahn M, Teschler-Nicola M, Kachhauser G, Plenk H. 1994. Age- and sex-dependent cancellous bone changes in a 4000y bp population. *Bone* 15:539–545.
- Kothari M, Keaveny TM, Lin JC, Newitt DC, Genant HK, Majumdar S. 1998. Impact of spatial resolution on the prediction of trabecular architecture parameters. *Bone* 22:437–443.
- Kuhn JL, Goldstein SA, Feldkamp LA, Goulet RW, Jesion G. 1990. Evaluation of a microcomputed tomography system to study trabecular bone structure. *J Orthop Res* 8:833–842.
- Kuo AD, Carter DR. 1991. Computational methods for analyzing the structure of cancellous bone in planar sections. *J Orthop Res* 9:918–931.
- Lanyon LE. 1974. Experimental support for the trajectorial theory of bone structure. *J Bone Joint Surg [Br]* 56:160–166.
- Layton MW, Goldstein SA, Goulet RW, Feldkamp LA, Kubinski DJ, Bole GG. 1988. Examination of subchondral bone architecture in experimental osteoarthritis by microscopic computed axial tomography. *Arthritis Rheum* 31:1400–1405.
- Lees CJ, Jerome CP. 1998. Effects of pregnancy and lactation on bone in cynomolgus macaques: histomorphometric analysis of iliac biopsies. *Bone* 22:545–549.
- Macchiarelli R, Bondioli L, Galichon V, Tobias PV. 1999. Hip bone trabecular architecture shows uniquely distinctive locomotor behaviour in South African australopithecines. *J Hum Evol* 36:211–232.
- Majumdar S, Genant HK, Grampp S, Newitt DC, Truong V-H, Lin JC, Mathur A. 1997. Correlation of trabecular bone structure with age, bone mineral density, and osteoporotic status: in vivo studies in the distal radius using high resolution magnetic resonance imaging. *J Bone Miner Res* 12:111–118.
- Martin RB. 1991. Determinants of the mechanical properties of bones. *J Biomech* 24:79–88.
- Martin RB, Burr DB, Sharkey NA. 1998. *Skeletal tissue mechanics*. New York: Springer.
- Mellish RWE, Garrahan NJ, Compston JE. 1989. Age-related changes in trabecular width and spacing in human iliac crest biopsies. *Bone Miner* 6:331–338.
- Mittermeier RA. 1978. Locomotion and postures in *Ateles geoffroyi* and *Ateles paniscus*. *Folia Primatol (Basel)* 30:161–193.
- Mosekilde L. 1989. Sex differences in age-related loss of vertebral trabecular bone mass and structure—biomechanical consequences. *Bone* 10:425–432.
- Mullender MG, Huiskes R, Versleyen H, Buma P. 1996. Osteocyte density and histomorphometric parameters in cancellous bone of the proximal femur in five mammalian species. *J Orthop Res* 14:972–979.
- Müller R, Koller B, Hildebrand T, Laib A, Gionollini S, Rügsegger P. 1996. Resolution dependency of microstructural properties of cancellous bone based on three-dimensional μ -tomography. *Tech Health Care* 4:113–119.
- Müller R, Van Campenhout H, Van Damme B, Van der Perre G, Dequeker T, Hildebrand T, Rügsegger P. 1998. Morphometric analysis of human bone biopsies: a quantitative structural comparison of histological sections and micro-computed tomography. *Bone* 23:59–66.
- Odgaard A. 1997. Three-dimensional methods for quantification of cancellous bone architecture. *Bone* 20:315–328.
- Odgaard A, Jensen EB, Gundersen HJG. 1990. Estimation of structural anisotropy based on volume orientation. A new concept. *J Microsc* 157:149–162.
- Odgaard A, Kabel J, van Rietbergen B, Dalstra M, Huiskes R. 1997. Fabric and elastic principal directions of cancellous bone are closely related. *J Biomech* 30:487–495.
- Ott SM, Lipkin EW, Newell-Morris L. 1999. Bone physiology during pregnancy and lactation in young macaques. *J Bone Miner Res* 14:1779–1788.
- Oxnard CE, Yang HC. 1981. Beyond biometrics: studies of complex biological patterns. *Symp Zool Soc Lond* 46:127–167.
- Parsons TJ, van Dusseldorp M, van der Vliet M, van de Werken K, Schaafsma G, van Staveren W. 1997. Reduced bone mass in Dutch adolescents fed a macrobiotic diet in early life. *J Bone Miner Res* 12:1486–1494.
- Pauwels F. 1960. *Biomechanics of the locomotor apparatus*. Berlin: Springer.
- Pope NS, Gould KG, Anderson DC, Mann DR. 1989. Effects of age and sex on bone density in the rhesus monkey. *Bone* 10:109–112.
- Rafferty KL. 1996. Joint design in primates: external and subarticular properties in relation to body size and locomotor behavior. Dissertation, Johns Hopkins University.
- Rafferty KL. 1998. Structural design of the femoral neck in primates. *J Hum Evol* 34:361–384.
- Rafferty KL, Ruff CB. 1994. Articular structure and function in *Hylobates*, *Colobus*, and *Papio*. *Am J Phys Anthropol* 94:395–408.
- Rawlins RG. 1976. Locomotor ontogeny in *Macaca mulatta*: I. Behavioral strategies and tactics. *Am J Phys Anthropol [Suppl]* 44:201.
- Rice JC, Cowin SC, Bowman JA. 1988. On the dependence of the elasticity and strength of cancellous bone on apparent density. *J Biomech* 21:155–168.
- Rook L, Bondioli L, Köhler M, Moyà-Solà S, Macchiarelli R. 1999. *Oreopithecus* was bipedal ape after all: evidence from the iliac cancellous architecture. *Proc Natl Acad Sci USA* 96:8795–8799.
- Rose MD. 1977. Positional behavior of olive baboons (*Papio ursinus*) and its relationship to maintenance and social activities. *Primates* 18:59–116.
- Ryan TM. 2000. Quantitative analysis of trabecular bone structure in the femur of lorisooid primates using high resolution x-ray computed tomography. *Am J Phys Anthropol [Suppl]* 30:266–267.

- Rüegsegger P, Koller B, Müller R. 1996. A microtomographic system for the nondestructive evaluation of bone architecture. *Calcif Tissue Int* 58:24–29.
- Smit THH, Schneider E, Odgaard A. 1998. Star length distribution: a volume-based concept for the characterization of structural anisotropy. *J Microsc* 191:249–257.
- Smith RJ, Jungers WL. 1997. Body mass in comparative primatology. *J Hum Evol* 32:523–559.
- Spoor CF, Wood B, Zonneveld F. 1994. Implications of early hominid labyrinthine morphology for evolution of human bipedal locomotion. *Nature* 369:645–648.
- Spoor F, Zonneveld F. 1995. Morphometry of the primate bony labyrinth—a new method based on high-resolution computed-tomography. *J Anat* 186:271–286.
- Swartz SM, Parker A, Huo C. 1998. Theoretical and empirical scaling patterns and topological homology in bone trabeculae. *J Exp Biol* 201:573–590.
- Tate JR, Cann CE. 1982. High-resolution computed tomography for the comparative study of fossil and extant bone. *Am J Phys Anthropol* 58:67–73.
- Teng S, Herring SW. 1995. A stereological study of trabecular architecture in the mandibular condyle of the pig. *Arch Oral Biol* 40:299–310.
- Thompson JL, Illerhaus B. 1998. A new reconstruction of the Le Moustier 1 skull and investigation of internal structures using 3-D- μ CT data. *J Hum Evol* 35:647–665.
- Turner CH. 1992. On Wolff's law of trabecular architecture. *J Biomech* 25:1–9.
- Turner CH, Cowin SC, Rho JY, Ashman RB, Rice JC. 1990. The fabric dependence of the orthotropic elastic constants of cancellous bone. *J Biomech* 23:549–561.
- Ulrich D, van Rietbergen B, Laib A, Rüegsegger P. 1999. The ability of three-dimensional structural indices to reflect mechanical aspects of trabecular bone. *Bone* 25:55–60.
- Whitehouse WJ. 1974. The quantitative morphology of anisotropic trabecular bone. *J Microsc* 101:153–168.
- Whitehouse WJ. 1975. Scanning electron micrographs of cancellous bone from the human sternum. *J Pathol* 116:213–224.
- Whitehouse WJ, Dyson ED. 1974. Scanning electron microscope studies of trabecular bone in the proximal end of the human femur. *J Anat* 118:417–444.